

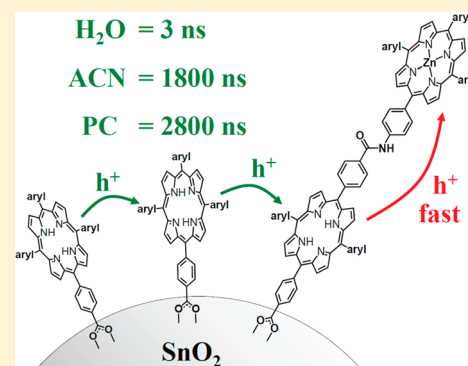
Solvent Dependence of Lateral Charge Transfer in a Porphyrin Monolayer

Bradley J. Brennan,[†] Kevin P. Regan, Alec C. Durrell, Charles A. Schmuttenmaer, and Gary W. Brudvig^{*†}

Department of Chemistry and Yale Energy Sciences Institute, Yale University, New Haven, Connecticut 06520-8107, United States

S Supporting Information

ABSTRACT: Lateral charge transport in a redox-active monolayer can be utilized for solar energy harvesting. A model porphyrin system was chosen to study the influence of the solvent on lateral hole hopping, which plays a crucial role in the charge-transfer kinetics. We examined the influence of water, acetonitrile, and propylene carbonate as solvents. Hole-hopping lifetimes varied by nearly 3 orders of magnitude among solvents, ranging from 3 ns in water to 2800 ns in propylene carbonate, and increased nonlinearly as a function of added acetonitrile in aqueous solvent mixtures. These results elucidate the important roles of solvation, molecular packing dynamics, and lateral charge-transfer mechanisms that have implications for all dye-sensitized photoelectrochemical device designs.



Surface-bound monolayers of redox active molecules on semiconductors are known to transport charges laterally along the surface.^{1–4} This property has been studied and exploited for various uses, namely in relation to molecular dye-sensitized semiconductors for solar energy conversion.^{5–14} In these systems, photoexcitation of the dye induces electron transfer to the n-type semiconductor, leaving an electron hole on the molecule. This hole can diffuse among the surface-bound molecules in competition with electron recombination processes. Recent reviews discuss current developments in this research area.^{15,16}

In solid-state dye-sensitized solar cells, lateral hole diffusion allows charges to more efficiently access the hole-transport species, generally Spiro-MeOTAD.⁸ In photoelectrocatalytic cells, lateral hole transport facilitates oxidation of a catalyst dispersed among the dyes.^{7,17} The surface-bound monolayer functions as a light-harvesting system and electronically connects the catalyst to multiple dye molecules. Lateral charge transport is a promising route toward overcoming the diffuse nature of sunlight and low efficiencies in multielectron photoelectrocatalytic cell designs.^{18–20} Under standard AM1.5G sunlight, which corresponds to 100 mW/cm², a dye absorbs approximately one photon per second,^{21,22} with photoinduced charges recombining orders of magnitude faster.²³ Therefore, in order to use sunlight to perform a multielectron catalytic reaction such as the four-electron oxidation of water, a significant number of dyes must work in conjunction with a single catalyst. Maximizing lateral charge-transport rates is thus essential to increasing solar photoelectrocatalytic device efficiencies.

In a dye–catalyst monolayer system, faster lateral charge transport competes more effectively with charge recombination

between the photoexcited electron and oxidized dye, allowing a larger number of dye molecules to electronically access a single catalyst. In past work, we developed a porphyrin system to study the various factors affecting lateral charge transfer.¹ Our design in Figure 1 depicts a light absorbing monolayer of freebase porphyrin (monomer H₂PF₈) on a SnO₂ nanoparticulate film. Randomly dispersed among this monolayer are porphyrin dyads consisting of a surface-bound freebase porphyrin with an appended zinc porphyrin (dyad, H₂PF₈–ZnPF₈) that act as thermodynamic sinks for the hole, similar to a catalyst. Previous research has shown that photons absorbed by ZnPF₈ efficiently transfer that energy to the freebase moiety.¹ The photoexcited H₂PF₈ monomer or dyad moiety (1) transfers an electron to the SnO₂ conduction band (2), yielding a charge-separated state with a conduction band electron and porphyrin radical cation (hole). The hole is then able to hop among neighboring porphyrins (3) in competition with recombination processes. Hole transfer to the H₂PF₈ moiety of the dyad results in intramolecular charge transfer to the zinc porphyrin on the subnanosecond time scale (4). The hole is then trapped and undergoes normal recombination processes with a semiconductor electron.

Using nanosecond transient absorption spectroscopy (ns-TAS), we were able to monitor the relative ratios of oxidized freebase and zinc porphyrin species in the monolayer as a function of time, which can be simulated using a hole-transfer model (see the Supporting Information for model description

Received: November 6, 2016

Accepted: December 19, 2016

Published: December 19, 2016

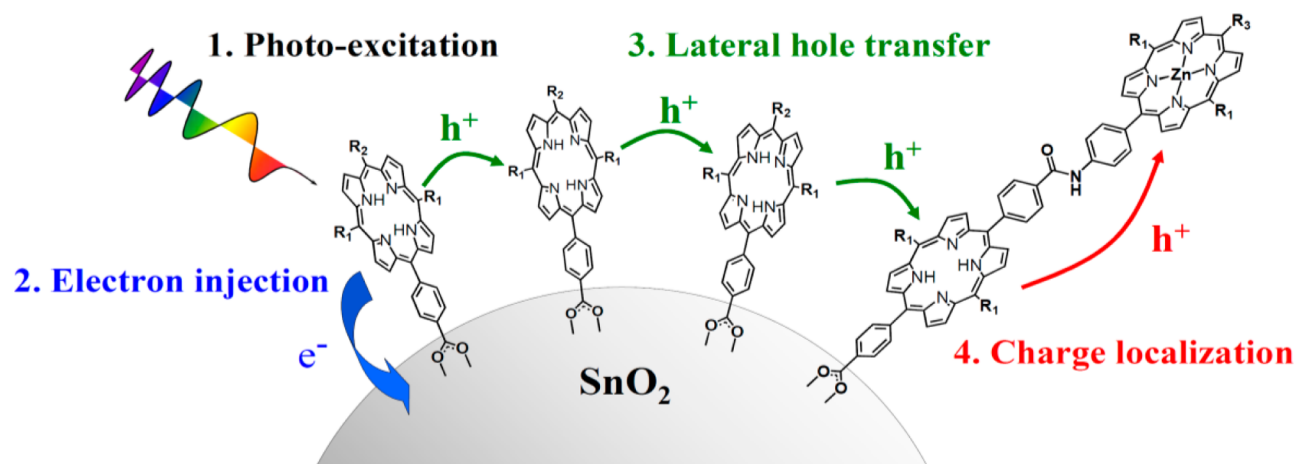


Figure 1. Model system for studying lateral charge transport. R_1 = 2,3,5,6-tetrafluorophenyl; R_2 = 4-carbomethoxyphenyl; R_3 = 4-trifluoroacetamidophenyl.

and limitations). We previously analyzed different ratios of monomer and dyad porphyrin monolayers ($\sim 90\%$ theoretical monolayer surface coverage) on SnO_2 films under aqueous conditions.¹ Our model indicated that lateral hole diffusion across the freebase porphyrin monolayer occurs via a random-walk process. While this was expected, the rate of $4.0 \times 10^7 \text{ s}^{-1}$ ($\tau = 25 \text{ ns}$) for each hole-hopping event was unexpectedly fast. The lateral hole-hopping rates were closer to those for intramolecular charge transfer rather than an intermolecular process²⁴ and outside the range of lateral hole-hopping rates studied in other porphyrin and ruthenium polypyridyl systems. In those studies, hole-hopping lifetimes ranged between hundreds of nanoseconds for the fastest systems to systems where no lateral transfer was observed at all.^{2,6,10} Two major differences between our system and others are: (1) we used SnO_2 instead of TiO_2 because the thermodynamics of our dyes for water oxidation devices require a lower conduction band minimum and (2) we performed our measurements in aqueous electrolyte while others use organic solvents, typically acetonitrile. These could lead to inherent differences in surface solvation, packing, and interporphyrin distances, all of which affect electron-transfer processes. To provide a better comparison with other studies, and to help elucidate the reasons for our observation of faster lateral hole-hopping rates, we studied the solvent dependence of the kinetics in our model system.

Monolayer samples with a 25:1 ratio of H_2PF_8 (monomer) to H_2PF_8 - ZnPF_8 (dyad) were prepared. At this ratio, we can use ns-TAS to study lateral charge-transfer rates ranging from reciprocal nanoseconds to reciprocal milliseconds. Ultraviolet (UV)-visible spectra of the molecules and the dye-sensitized SnO_2 films are shown in Figure 2. Slight spectral shifts between the solution and dry surface-bound material are expected and observed, and it is apparent that there is only a small percentage of dyad on the surface (see Figure S2).

The samples were immersed in different solvents [water, acetonitrile (ACN), water/acetonitrile mixtures (vol %), and propylene carbonate (PC)] containing 100 mM LiClO_4 as electrolyte. They were analyzed by using ns-TAS, which entailed photoexciting the samples with 515 nm light and probing at 560 nm. The freebase H_2PF_8 is primarily photoexcited at the chosen pump wavelength and injects an electron into the SnO_2 conduction band. The ns-TAS signature

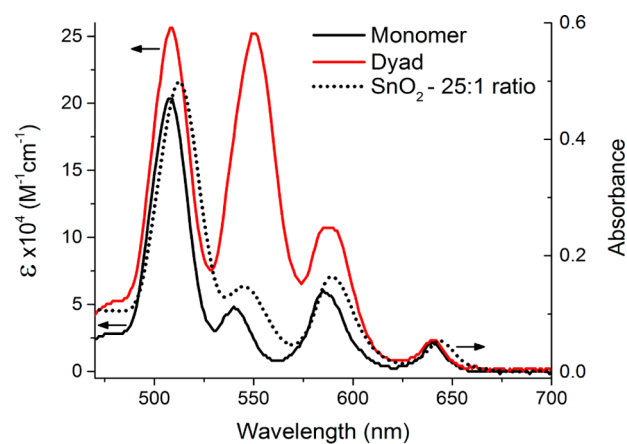


Figure 2. UV-visible spectra in the Q-band region of model porphyrins in solution and dye-sensitized SnO_2 . Spectra of monomer (black solid line) and dyad (red solid line) in ethyl acetate solvent were obtained from ref 1, and the absorbance of a 25:1 monomer-to-dyad sample was obtained using a dry SnO_2 film (black dotted line).

of the H_2PF_8 radical cation (hole) shown in Figure 3 is then observed as a positive value at the probe wavelength. The hole randomly traverses the monolayer (unobservable by TAS) and can either recombine with SnO_2 conduction band electrons or

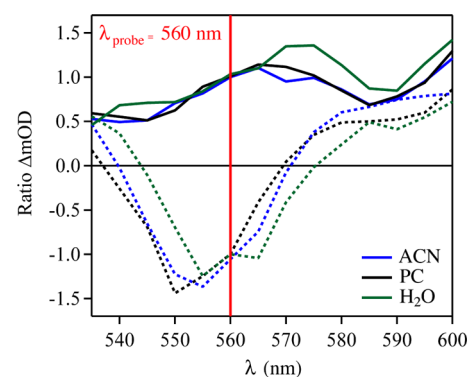


Figure 3. TA map of monomer (solid lines) and dyad (dashed lines) porphyrin radical cations. Data were normalized at the probe wavelength of 560 nm.

reside on the H_2PF_8 moiety of a dyad, in which case rapid intramolecular charge transfer produces the ZnPF_8 radical cation, which has a negative TA signature at 560 nm due to a bleach of the zinc porphyrin Q-band. The trapped hole on ZnPF_8 then undergoes recombination and the signal decays. The observed signal as a function of delay time is the sum of H_2PF_8 and ZnPF_8 radical cation contributions. The ratio of extinction coefficients at 560 nm for the ZnPF_8 (negative signal) and H_2PF_8 (positive signal) porphyrin radical cations was previously determined to be -3.5 .¹

Monolayers of pure monomer or dyad on SnO_2 in each solvent were analyzed by ns-TAS to determine their recombination rates (see Figure S3). The decay of signal due to recombination at early delay times is well-described by a stretched exponential decay function corresponding to the Kohlrausch–Williams–Watts (KWW) kinetic model, which is commonly used for molecular dyes on metal oxides.²⁵ Transient absorption spectra revealed only minor solvatochromic shifts among solvents (Figures 3 and S4).

For the mixed-species monolayers, it is apparent in Figure 4 that the ns-TAS signals transition from positive values toward

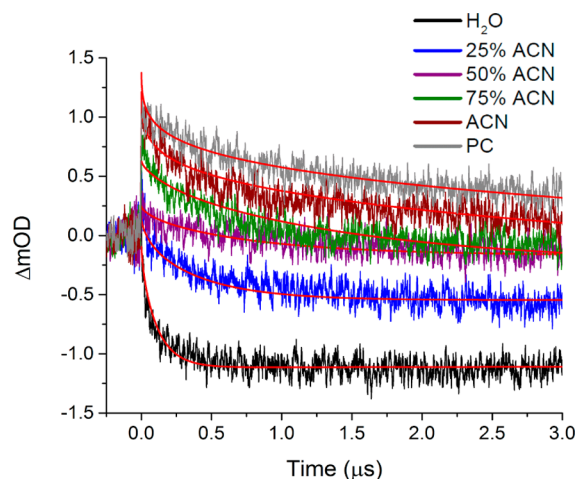


Figure 4. Transient absorption spectra of dye-sensitized SnO_2 films with porphyrin monolayers containing 25:1 monomer-to-dyad ratio in different solvents. Fits (red) were obtained using the model described in the text and the kinetic parameters in Table 1.

negative values much faster for samples in water than those with added acetonitrile or in the pure organic solvents. Signals for all solvents eventually become negative before decaying back toward the baseline by recombination processes (see Figure S5). As was observed previously,¹ the dyad has different recombination kinetics when dispersed in a H_2PF_8 monomer monolayer compared to a pure monolayer of dyad, and this is the case in all the solvents examined in this study. The ZnPF_8 solvation sphere is entirely that of solvent when dispersed in a monolayer of H_2PF_8 monomer, while in the pure monolayer of dyad it is surrounded by other ZnPF_8 moieties. This solvent accessibility leads to a much slower recombination rate in the more isolated dyads.²¹

Data shown in Figure 4, along with the recombination kinetics for both monomer and dyad, were input into a random-walk model previously described to simulate the transient absorption spectra and calculate the hole-hopping rate.¹ The fits are presented in Figure 4, with a longer time window shown in Figure S5. The observed hole-hopping

lifetimes are presented in Table 1. The stretched exponential decay recombination dynamics were relatively consistent

Table 1. Lateral Charge-Transfer Rates and Model Kinetic Parameters^a

solvent	k_{hop} (sec^{-1})	τ_{hop} (ns)	$k_{\text{rec,mono}}$ (sec^{-1})	β_{mono}	$k_{\text{rec,dyad}}$ (sec^{-1})	β_{dyad}
H_2O	3.6×10^8	3	1.3×10^5	0.25	2300	1.0
25% ACN	8.9×10^7	11	1.3×10^6	0.25	1500	1.0
50% ACN	5.0×10^7	20	1.0×10^5	0.20	1200	1.0
75% ACN	2.5×10^7	40	8.0×10^5	0.25	1000	1.0
ACN	5.6×10^5	1800	4.0×10^5	0.23	700	1.0
PC	3.6×10^5	2800	2.6×10^5	0.25	500	1.0

^aAcetonitrile solvent mixtures with water are volume %.

among solvents. For the monomer, values of β vary between 0.20 and 0.25, and recombination rates vary between 1.0×10^5 and $1.3 \times 10^6 \text{ s}^{-1}$. For the dyad, recombination rates vary between 0.5×10^3 and $2.3 \times 10^3 \text{ s}^{-1}$ with a fixed β value of 1 corresponding to a single exponential decay in the KWW model.

While recombination rates are similar among solvents, the hole-hopping lifetimes span nearly 3 orders of magnitude from 3 to 2800 ns. We obtain 3 ns per hop in water, which is similar to our previously published value (25 ns),¹ and the hole-hopping lifetime increases significantly as the proportion of acetonitrile is increased. The results in acetonitrile (1800 ns) and propylene carbonate (2800 ns), which are polar organic solvents, are similar to each other. This contrasts with previous reports in the literature, as comparable rates are obtained for ruthenium bipyridine analogs in both water and acetonitrile.^{5,26}

The wide range of calculated lateral charge-transfer rates in the water/acetonitrile mixtures provides insight into the dynamics. According to Marcus theory of electron transfer in a classical nonadiabatic system, electron self-exchange rates are strongly dependent on the solvent because of inherent differences in outer-sphere reorganization energies.^{27,28} The rate, k , of electron self-exchange (i.e., when $\Delta G^\circ = 0$) is described in its most general form in eq 1 as

$$k = \frac{2\pi}{\hbar} |V|^2 \frac{1}{\sqrt{4\pi\lambda k_b T}} \exp\left(-\frac{\lambda}{4k_b T}\right) \quad (1)$$

This relates the rate of electron transfer (k) to the electronic coupling (V) between the donor and acceptor, the reorganization energy of the reaction (λ), the Boltzmann constant (k_b), and the temperature (T). In solvents with higher polarity, λ generally increases, causing k to decrease. Our results are the opposite of this general trend and complement recent results by Moia and co-workers using a different molecular system.¹⁴

Multiple explanations can be hypothesized for the unexpected results, but most can be discounted outright because of the magnitude of the change in hole-hopping rates. One possible explanation for the wide discrepancy is solvent-dependent ion pairing of the H_2PF_8 moiety. Ion pairing is a complicated phenomenon that has been theorized and experimentally observed to significantly affect charge-transfer rates by increasing outer-sphere reorganizational energies.^{29–34} The strength of ion pairing correlates with spectral shifting of the ion, in this case that of the monomer porphyrin radical

cation shown in Figure S4. The relatively minor observed spectral shift of 5–10 nm among the solvents containing LiClO₄ electrolyte can be attributed to general solvatochromism. Therefore, ion pairing need not be considered as a possibility in our system.^{35,36}

We believe hydrophobic clustering provides the simplest explanation for the significant differences in solvent-dependent hole-hopping rates. Shown in Figure 5, hydrophobic clustering

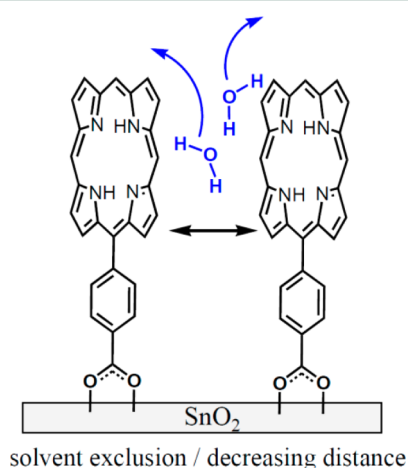


Figure 5. Hydrophobic clustering. Porphyrin aryl substituents are removed for clarity.

occurs when water is excluded from the solvation sphere of the largely hydrophobic porphyrin. Because the porphyrin is not soluble in water, and the surface-anchoring carboxylic acid has been shown to be unstable,^{37,38} the porphyrins could undergo a hydrophobic collapse into a more well-packed monolayer, thereby excluding solvent waters. This solvent exclusion process could be driven by the entropy gained from the loss of solvation waters, similar to micellization.³⁹ Thus, in water, the porphyrins are actually solvated by the relatively nonpolar appendages of the surrounding porphyrins, a conclusion supported by our results that agrees with Marcus electron-transfer theory.

In addition to merely altering the solvation environment, rearrangement to a more well-packed monolayer would decrease the distance between porphyrins. While previous results have shown that the initially formed monolayer is relatively well-packed,¹ removing a single shell of hydration or even interstitial solvent molecules from each porphyrin would decrease the interporphyrin tunneling distance by a significant amount. These two factors both exponentially increase the charge-transfer rate according to the Marcus theory of electron transfer and can account for the wide range of hole-hopping rates in the solvent systems.²⁸

The generalized form of Marcus electron-transfer theory in eq 1 can be further differentiated for our specific case. Equations 2 and 3 provide a summary of the effects of distance, tunneling medium, and reorganizational energies on electron-transfer rates. In eq 2, the electronic coupling matrix element (V), which is directly proportional to the rate of electron transfer (k), increases exponentially with decreasing distance (R) between porphyrins beyond van der Waals separation (R_0).²⁸ Altering the solvation environment also modifies the medium-dependent scalar for electron tunneling (β_T), which becomes smaller in more nonpolar solvents, further increasing the electron-transfer rate as water is replaced by a

less polar environment.⁴⁰ In eq 3, k is also exponentially dependent on the reorganizational energy (λ), which is generally dominated by outer-sphere solvent dynamics.⁴¹ If solvent is excluded and replaced by rigid aryl functionalities, a significant decrease in λ is expected with a concomitant increase in k . A caveat to this assessment is the unknown nature of the metal oxide surface, where solvation and surface potentials could affect the local environment around the porphyrin.

$$k \propto V \propto \exp\left(-\frac{\beta_T(R - R_0)}{2}\right) \quad (2)$$

$$k \propto \exp\left(-\frac{\lambda}{4}\right) \quad (3)$$

Our results in the pure organic solvents, which we believe solvate porphyrins in a more ideal way, allow direct comparison to hole-hopping kinetics in other model systems using porphyrins or inorganic coordination complexes. The average hole-hopping lifetimes in acetonitrile and propylene carbonate of 1800 and 2800 ns, respectively, are similar to that observed by others.^{2,6} Thus, our results in aqueous solutions are extraordinary, while those in organic solvents are fairly typical. Because of the similarity of the lifetimes in these pure organic solvents, there is not enough information to conclusively show that the system follows classical Marcus theory where charge-transfer rates increase with decreasing solvent Pekar factor (given by $1/\epsilon_\infty - 1/\epsilon_0$, and is 0.53 for acetonitrile and 0.48 for propylene carbonate) or with decreasing solvent longitudinal relaxation time (acetonitrile, 0.2×10^{-12} s; propylene carbonate, 2.6×10^{-12} s).⁴² Lifetimes measured in additional organic solvents would be needed, but these initial results suggest it is the latter.

From the lateral charge-transfer model, we can estimate the harvesting efficiency of the photoinduced charges by determining the percentage of holes that become localized on the dyad prior to recombination. In the case of water, 77% of holes become localized while only 19% are localized in acetonitrile and 17% in propylene carbonate. The higher rate of lateral charge transfer under aqueous conditions makes the overall efficiency of hole hopping to the dyad relatively high. In a monolayer with porphyrin–dyad ratio of 2.5:1, a majority of the charge carriers produced by absorption of solar energy can be collected by the dyad which comprises less than 4% of the monolayer. This is an important result for the development of aqueous photoelectrocatalytic devices where multiple dyes must electronically interact with a single catalyst.

In summary, we describe the solvent dependence of lateral charge transfer in a porphyrin-based model system, generating new understanding of the roles of solvation and the complexity of surface dynamics on the kinetic rates. Our previous results suggesting relatively fast hole hopping in water have been confirmed with a lifetime of 3 ns in the system studied with aqueous LiClO₄ electrolyte, and this lifetime is shown to increase dramatically toward 1800 ns as the solvent fraction of acetonitrile is increased. Our hypothesis is that the porphyrin monolayer reorganizes to exclude solvent, thereby increasing the hole-hopping rate by decreasing the electron tunneling parameter (β_T), reorganizational energy (λ), and likely the intermolecular porphyrin distances. These results provide new insights into lateral charge-transfer mechanisms and are of interest to those studying redox-active monolayers in dye-sensitized systems. The results are particularly promising for

the prospect of exploiting lateral charge transfer in aqueous environments, such as photoelectrocatalytic water oxidation.

■ ASSOCIATED CONTENT

Supporting Information

The Supporting Information is available free of charge on the ACS Publications website at DOI: 10.1021/acsenergylett.6b00583.

Experimental procedures, description of the model, characterization of samples, and additional transient absorption data (PDF)

■ AUTHOR INFORMATION

Corresponding Author

*E-mail: gary.brudvig@yale.edu.

ORCID

Gary W. Brudvig: 0000-0002-7040-1892

Present Address

†B.J.B.: Department of Chemistry, California Institute of Technology, 1200 East California Boulevard, Pasadena, CA 91125.

Notes

The authors declare no competing financial interest.

■ ACKNOWLEDGMENTS

We heartily thank Rudy Marcus, Jay Winkler, and Harry Gray at Caltech for their fruitful discussions of the intricacies of electron transfer in complex systems. We also thank Gerald Meyer at the University of North Carolina—Chapel Hill for his helpful insights into our hole-hopping model. This work has been funded by the U.S. Department of Energy Office of Science, Office of Basic Energy Sciences, under Award DE-FG02-07ER15909 and by a generous donation from the TomKat Charitable Trust.

■ REFERENCES

- (1) Brennan, B. J.; Durrell, A. C.; Koepf, M.; Crabtree, R. H.; Brudvig, G. W. Towards Multielectron Photocatalysis: A Porphyrin Array for Lateral Hole Transfer and Capture on a Metal Oxide Surface. *Phys. Chem. Chem. Phys.* **2015**, *17*, 12728–12734.
- (2) Ardo, S.; Meyer, G. J. Characterization of Photoinduced Self-Exchange Reactions at Molecule–Semiconductor Interfaces by Transient Polarization Spectroscopy: Lateral Intermolecular Energy and Hole Transfer across Sensitized TiO₂ Thin Films. *J. Am. Chem. Soc.* **2011**, *133*, 15384–15396.
- (3) Heimer, T. A.; D'Arcangelis, S. T.; Farzad, F.; Stipkala, J. M.; Meyer, G. J. An Acetylacetonate-Based Semiconductor–Sensitizer Linkage. *Inorg. Chem.* **1996**, *35*, 5319–5324.
- (4) Bonhôte, P.; Gogniat, E.; Tingry, S.; Barbé, C.; Vlachopoulos, N.; Lenzenmann, F.; Comte, P.; Grätzel, M. Efficient Lateral Electron Transport inside a Monolayer of Aromatic Amines Anchored on Nanocrystalline Metal Oxide Films. *J. Phys. Chem. B* **1998**, *102*, 1498–1507.
- (5) Wang, Q.; Zakeeruddin, S. M.; Nazeeruddin, M. K.; Humphry-Baker, R.; Graetzel, M. Molecular Wiring of Nanocrystals: NCS-Enhanced Cross-Surface Charge Transfer in Self-Assembled Ru-Complex Monolayer on Mesoscopic Oxide Films. *J. Am. Chem. Soc.* **2006**, *128*, 4446–4452.
- (6) Hu, K.; Robson, K. C. D.; Beauvilliers, E. E.; Schott, E.; Zarate, X.; Arratia-Perez, R.; Berlinguette, C. P.; Meyer, G. J. Intramolecular and Lateral Intermolecular Hole Transfer at the Sensitized TiO₂ Interface. *J. Am. Chem. Soc.* **2014**, *136*, 1034–1046.
- (7) Song, W.; Ito, A.; Binstead, R. A.; Hanson, K.; Luo, H.; Brennaman, M. K.; Concepcion, J. J.; Meyer, T. J. Accumulation of

Multiple Oxidative Equivalents at a Single Site by Cross-Surface Electron Transfer on TiO₂. *J. Am. Chem. Soc.* **2013**, *135*, 11587–11594.

(8) Moia, D.; Cappel, U. B.; Leijtens, T.; Li, X.; Telford, A. M.; Snaith, H. J.; O'Regan, B. C.; Nelson, J.; Barnes, P. R. F. The Role of Hole Transport between Dyes in Solid-State Dye-Sensitized Solar Cells. *J. Phys. Chem. C* **2015**, *119*, 18975–18985.

(9) Moia, D.; Vaissier, V.; López-Duarte, I.; Torres, T.; Nazeeruddin, M. K.; O'Regan, B. C.; Nelson, J.; Barnes, P. R. F. The Reorganization Energy of Intermolecular Hole Hopping between Dyes Anchored to Surfaces. *Chem. Sci.* **2014**, *5*, 281–290.

(10) Vaissier, V.; Barnes, P.; Kirkpatrick, J.; Nelson, J. Influence of Polar Medium on the Reorganization Energy of Charge Transfer between Dyes in a Dye Sensitized Film. *Phys. Chem. Chem. Phys.* **2013**, *15*, 4804–4814.

(11) Vaissier, V.; Frost, J. M.; Barnes, P. R. F.; Nelson, J. Influence of Intermolecular Interactions on the Reorganization Energy of Charge Transfer between Surface-Attached Dye Molecules. *J. Phys. Chem. C* **2015**, *119*, 24337–24341.

(12) Vaissier, V.; Mosconi, E.; Moia, D.; Pastore, M.; Frost, J. M.; De Angelis, F.; Barnes, P. R. F.; Nelson, J. Effect of Molecular Fluctuations on Hole Diffusion within Dye Monolayers. *Chem. Mater.* **2014**, *26*, 4731–4740.

(13) DiMarco, B. N.; Motley, T. C.; Balok, R. S.; Li, G.; Siegler, M. A.; O'Donnell, R. M.; Hu, K.; Meyer, G. J. A Distance Dependence to Lateral Self-Exchange across Nanocrystalline TiO₂. A Comparative Study of Three Homologous Ru(II)/II Polypyridyl Compounds. *J. Phys. Chem. C* **2016**, *120*, 14226–14235.

(14) Moia, D.; Szumska, A.; Vaissier, V.; Planells, M.; Robertson, N.; O'Regan, B. C.; Nelson, J.; Barnes, P. R. F. Inter-Dye Hole Transport Accelerates Recombination in Dye Sensitized Mesoporous Films. *J. Am. Chem. Soc.* **2016**, *138*, 13197–13206.

(15) Pastore, M.; Etienne, T.; De Angelis, F. Structural and Electronic Properties of Dye-Sensitized TiO₂ for Solar Cell Applications: From Single Molecules to Self-Assembled Monolayers. *J. Mater. Chem. C* **2016**, *4*, 4346–4373.

(16) Hu, K.; Meyer, G. J. Lateral Intermolecular Self-Exchange Reactions for Hole and Energy Transport on Mesoporous Metal Oxide Thin Films. *Langmuir* **2015**, *31*, 11164–11178.

(17) Ardo, S.; Meyer, G. J. Direct Observation of Photodrivern Intermolecular Hole Transfer across TiO₂ Nanocrystallites: Lateral Self-Exchange Reactions and Catalyst Oxidation. *J. Am. Chem. Soc.* **2010**, *132*, 9283–9285.

(18) Youngblood, W. J.; Lee, S. A.; Kobayashi, Y.; Hernandez-Pagan, E. A.; Hoertz, P. G.; Moore, T. A.; Moore, A. L.; Gust, D.; Mallouk, T. E. Photoassisted Overall Water Splitting in a Visible Light-Absorbing Dye-Sensitized Photoelectrochemical Cell. *J. Am. Chem. Soc.* **2009**, *131*, 926–927.

(19) Moore, G. F.; Blakemore, J. D.; Milot, R. L.; Hull, J. F.; Song, H.; Cai, L.; Schmuttenmaer, C. A.; Crabtree, R. H.; Brudvig, G. W. A Visible Light Water-Splitting Cell with a Photoanode Formed by Codeposition of a High-Potential Porphyrin and an Iridium Water-Oxidation Catalyst. *Energy Environ. Sci.* **2011**, *4*, 2389–2392.

(20) Swierk, J. R.; Méndez-Hernández, D. D.; McCool, N. S.; Liddell, P.; Terazono, Y.; Pahk, I.; Tomlin, J. J.; Oster, N. V.; Moore, T. A.; Moore, A. L.; et al. Metal-Free Organic Sensitizers for Use in Water-Splitting Dye-Sensitized Photoelectrochemical Cells. *Proc. Natl. Acad. Sci. U. S. A.* **2015**, *112*, 1681–1686.

(21) O'Regan, B. C.; Durrant, J. R. Kinetic and Energetic Paradigms for Dye-Sensitized Solar Cells: Moving from the Ideal to the Real. *Acc. Chem. Res.* **2009**, *42*, 1799–1808.

(22) McConnell, I.; Li, G.; Brudvig, G. W. Energy Conversion in Natural and Artificial Photosynthesis. *Chem. Biol.* **2010**, *17*, 434–447.

(23) Green, A. N. M.; Palomares, E.; Haque, S. A.; Kroon, J. M.; Durrant, J. R. Charge Transport Versus Recombination in Dye-Sensitized Solar Cells Employing Nanocrystalline TiO₂ and SnO₂ Films. *J. Phys. Chem. B* **2005**, *109*, 12525–12533.

(24) Holten, D.; Bocian, D. F.; Lindsey, J. S. Probing Electronic Communication in Covalently Linked Multiporphyrin Arrays. A Guide

to the Rational Design of Molecular Photonic Devices. *Acc. Chem. Res.* **2002**, *35*, 57–69.

(25) Abrahamsson, M.; Johansson, P. G.; Ardo, S.; Kopecky, A.; Galoppini, E.; Meyer, G. J. Decreased Interfacial Charge Recombination Rate Constants with N3-Type Sensitizers. *J. Phys. Chem. Lett.* **2010**, *1*, 1725–1728.

(26) Hanson, K.; Brennaman, M. K.; Ito, A.; Luo, H.; Song, W.; Parker, K. A.; Ghosh, R.; Norris, M. R.; Glasson, C. R. K.; Concepcion, J. J.; et al. Structure–Property Relationships in Phosphonate-Derivatized, R_{ii} Polypyridyl Dyes on Metal Oxide Surfaces in an Aqueous Environment. *J. Phys. Chem. C* **2012**, *116*, 14837–14847.

(27) Marcus, R. A.; Sutin, N. Electron Transfers in Chemistry and Biology. *Biochim. Biophys. Acta, Rev. Bioenerg.* **1985**, *811*, 265–322.

(28) Closs, G. L.; Miller, J. R. Intramolecular Long-Distance Electron Transfer in Organic Molecules. *Science* **1988**, *240*, 440–447.

(29) Marcus, Y.; Hefter, G. Ion Pairing. *Chem. Rev.* **2006**, *106*, 4585–4621.

(30) Saveant, J. M. Electron Hopping between Localized Sites: Effect of Ion Pairing on Diffusion and Migration; General Rate Laws and Steady-State Responses. *J. Phys. Chem.* **1988**, *92*, 4526–4532.

(31) Saveant, J. M. Electron Hopping between Localized Sites: Coupling with Electroinactive Counterion Transport. *J. Phys. Chem.* **1988**, *92*, 1011–1013.

(32) Marcus, R. A. Ion Pairing and Electron Transfer. *J. Phys. Chem. B* **1998**, *102*, 10071–10077.

(33) Vakarin, E. V.; Holovko, M. F.; Piotrowiak, P. Ion-Pairing Effects in Intramolecular Electron Transfer. *Chem. Phys. Lett.* **2002**, *363*, 7–12.

(34) Piotrowiak, P.; Miller, J. R. Counterion Effects in Intramolecular Charge Transfer in Radical Anions. *J. Phys. Chem.* **1993**, *97*, 13052–13060.

(35) Bottomley, L. A.; Kadish, K. M. Counterion and Solvent Effects on the Electrode Reactions of Iron Porphyrins. *Inorg. Chem.* **1981**, *20*, 1348–1357.

(36) Chang, D.; Malinski, T.; Ulman, A.; Kadish, K. M. Electrochemistry of Nickel(II) Porphyrins and Chlorins. *Inorg. Chem.* **1984**, *23*, 817–824.

(37) Brennan, B. J.; Llansola Portoles, M. J.; Liddell, P. A.; Moore, T. A.; Moore, A. L.; Gust, D. Comparison of Silatrane, Phosphonic Acid, and Carboxylic Acid Functional Groups for Attachment of Porphyrin Sensitizers to TiO₂ in Photoelectrochemical Cells. *Phys. Chem. Chem. Phys.* **2013**, *15*, 16605–16614.

(38) Brennan, B. J.; Keirstead, A. E.; Liddell, P. A.; Vail, S. A.; Moore, T. A.; Moore, A. L.; Gust, D. 1-(3'-Amino)Propylsilatrane Derivatives as Covalent Surface Linkers to Nanoparticulate Metal Oxide Films for Use in Photoelectrochemical Cells. *Nanotechnology* **2009**, *20*, 505203.

(39) Misra, P. K.; Mishra, B. K.; Behera, G. B. Micellization of Ionic Surfactants in Tetrahydrofuran-Water and Acetonitrile-Water Mixed-Solvent Systems. *Colloids Surf.* **1991**, *57*, 1–10.

(40) Gray, H. B.; Winkler, J. R. Long-Range Electron Transfer. *Proc. Natl. Acad. Sci. U. S. A.* **2005**, *102*, 3534–3539.

(41) Marcus, R. A. Electron Transfer Reactions in Chemistry. Theory and Experiment. *Rev. Mod. Phys.* **1993**, *65*, 599–610.

(42) Grampp, G.; Harrer, W.; Jaenicke, W. The Role of Solvent Reorganization Dynamics in Homogeneous Electron Self-Exchange Reactions. *J. Chem. Soc., Faraday Trans. 1* **1987**, *83*, 161–166.

Supporting Information

Solvent Dependence of Lateral Charge Transfer in a Porphyrin Monolayer

Bradley J. Brennan,^a Kevin P. Regan, Alec C. Durrell, Charles A. Schmuttenmaer, Gary W. Brudvig*

Department of Chemistry, and Yale Energy Sciences Institute, Yale University, New Haven, CT 06520-8107, USA.

^a Present address: Department of Chemistry, California Institute of Technology, 1200 East California Boulevard, Pasadena, CA 91125, United States

Corresponding Author

*E-mail: Gary.Brudvig@yale.edu

<u>Sample preparation</u>	page S2
<u>Transient absorption</u>	S2
<u>Summary of random-walk model</u>	S2
<u>Figure S1: Random-walk probability curves</u>	S3
<u>Figure S2. UV-visible spectra overlay of solution and dye-sensitized electrode</u>	S4
<u>Figure S3. Transient absorption spectra of monomer-sensitized SnO₂</u>	S5
<u>Figure S4. Transient absorption spectral map of monomer</u>	S6
<u>Figure S5. Transient absorption spectra of dye-sensitized SnO₂ electrodes in 25:1 ratio</u>	S6
<u>References</u>	S6

1) Sample Preparation

Synthesis and characterization of the porphyrins can be found in previously published work.¹ Nanoparticulate SnO₂ films on FTO-coated glass (TEC 15, Hartford Glass) were prepared by a doctor-blading method using SnO₂ colloidal paste composed of ~15 nm diameter SnO₂ nanoparticles (Alfa Aesar, Nanoarc) prepared using a previously published procedure.² The paste consisted of 10% SnO₂ and 5% ethyl cellulose in a mixture of water, acetic acid, and α -terpineol. Using a double-layered mask of Scotch Magic Tape, films of ~8 μ m were prepared prior to annealing in a programmable oven by ramping the temperature to 370 °C at 3 °C/minute, holding for 10 minutes, ramping to 470 °C at 3 °C/minute, holding for 30 minutes, and then slowly cooling. The transparent films were kept in a 120 °C oven until use.

The SnO₂ films on FTO were sensitized with a monolayer of porphyrin by soaking in a porphyrin / ethyl acetate solution for ~10 hours, and then rinsed in ethyl acetate. For pure monomer and dyad films, ~250 μ M porphyrin solutions in ethyl acetate were used, while the 25:1 monomer/dyad ratio monolayers were prepared using a mixed porphyrin solution containing a 25:1 ratio of monomer to dyad. Previous analysis has shown that the surface monolayers are composed of the same ratio as that of the soaking solution.¹ Steady-state UV-visible spectroscopy was performed using a Shimadzu UV-2600 spectrophotometer. SnO₂ thickness was determined using a Tencor Alpha-step 200 profilometer.

2) Transient Absorption

An Edinburgh Instruments LP900 transient absorption spectrometer was used for data collection. The samples were photoexcited with an ~7 ns pulse at 515 nm which was generated by an optical parametric oscillator (OPO, Spectra Physics) that was pumped with the third harmonic (355 nm) of a Nd:YAG laser (Spectra Physics INDI-10). The probe was generated by a pulsed 450 W Xe arc lamp that was filtered to selectively probe at the desired wavelength. Dye-sensitized SnO₂ films were held at a 45° angle relative to the pump and probe illumination paths in a 1 cm path length cuvette containing the experimental solvent and 100 mM LiClO₄. The pump power was 1 mJ/pulse for recombination kinetic experiments, and 200-400 μ J/pulse for data collection with the 25:1 monomer-to-dyad films. At this pump power, less than 1 in 25 dyes are theoretically photoexcited when reflections and scattering are taken into account. Signal intensity was linear with pump power in this regime, and hole-hopping kinetics were independent of pump power.

3) Summary of Random-Walk Model

Kinetic values for electron self-exchange were obtained using a previously discussed model.¹ This model effectively simulates the transient absorption spectrum by incorporating the known rates of electron-hole recombination on a photoactive surface monolayer (found from the spectral profiles of the dyes) and the calculated electron self-exchange (lateral hole-hopping) rate using a standard hexagonal random-walk model. The intramolecular rate of hole transfer within the dyad was modeled as an instantaneous process, as it is observed experimentally to occur on the sub-nanosecond timescale in all solvents.

Using a randomized, hexagonally packed system of monomer and dyad in a 25:1 ratio, a random-walk scenario was analyzed where a randomly assigned molecule (monomer/dyad) was chosen to initiate a photo-induced electron injection into the semiconductor, thereby becoming the oxidized porphyrin radical cation (hole). This hole was allowed to randomly hop among the porphyrins until it reached a dyad, and the number of required hops was logged. This scenario was repeated with 10^6 randomized systems producing the probability curve for reaching a dyad as a function of number of hops, and is shown in Figure S1.

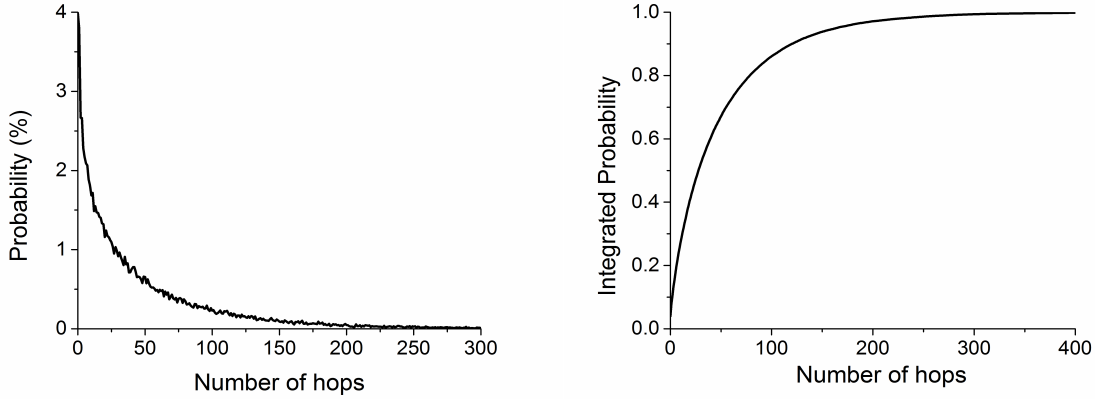


Figure S1: Random-walk probability curves. The probability density of reaching a dyad after each hop (left) and integrated probability (right). Data taken from reference S1.

The probability distributions from Figure S1 allow for modeling of the photoactive surface as a sum of monomers (M) which are some number of hops (n) from reaching a dyad as is shown in Equations S1-S3. For calculations, n was limited to 300, which effectively incorporates over 99% of the possible holes.

$$[M_{\text{total}}] = [M_1] + [M_2] + [M_3] + \dots + [M_n] \quad (\text{S1})$$

$$-\frac{d[M_n]}{dt} = [(\beta_M k_{\text{rec},M}^{\beta_M} t^{\beta_M-1} + k_{\text{hop}})[M_n]] - k_{\text{hop}}[M_{n+1}] \quad (\text{S2})$$

$$-\frac{d[D]}{dt} = [(\beta_D k_{\text{rec},D}^{\beta_D} t^{\beta_D-1})[D]] - k_{\text{hop}}[M_1] \quad (\text{S3})$$

Incorporation of the known charge-recombination parameters (stretched-exponential decay from the pure monomer and dyad films) with the random-walk probability distributions provides a means to determine the relative oxidized monomer and dyad populations as a function of time (Equation S2 and S3). The oxidized monomer species are separated by their total number of hops (n) from the dyad. In Equation S2, the change in population for oxidized monomer species which are n hops from a dyad is dependent on the initial population of M_n , the rate of recombination (stretched exponential decay), k_{hop} , and the population of M which is $n+1$ hops from the dyad. M_n decreases with recombination events, decreases as holes hop towards a dyad, and increases as the population transfers from M_{n+1} to M_n . The populations of M can be summed for any time period using Equation S1. In Equation S3, the change in population of dyad (D) is decreased with recombination events and increased as holes hop from the M_1 population which is only a single hop from the dyad. No further lateral charge transfer is considered once the hole is located on a dyad.

Using the populations of M and D at any point in time, and the known ratio of monomer and dyad transient absorption intensities at the observed wavelength (~ 3.5 at 560 nm), Equation S4 can simulate the transient absorption (ΔOD) signal with scaling factor A and can account for any minor offsets (b). The experimental transient absorption spectra were simulated from Equation S4 using the populations of M and D obtained as a function of the variable k_{hop} .

$$\Delta OD = A([M]_t + \varepsilon[D]_t) + b \quad (S4)$$

Limitations of the model. The derivations using stretched exponential recombination kinetics as the method of incorporating time into the model resulted in factors of t^{-1} in Equations S2 and S3. Since β must be between 0 and 1, this effectively puts time in the denominator. Thus, the calculations will break down at ultrafast time regimes where t is very small, generally on the femtosecond timescale. For our calculations, which are on orders of magnitude longer timescales, we exclude the first 1 ns of transient absorption kinetic data and start our calculations at $t \sim 1$ ns to place ourselves well within the time window where the equations converge and fit the data. Exclusion of the data does not affect our results, as the great majority of the transient absorption decay takes place on timescales that are orders of magnitude longer.

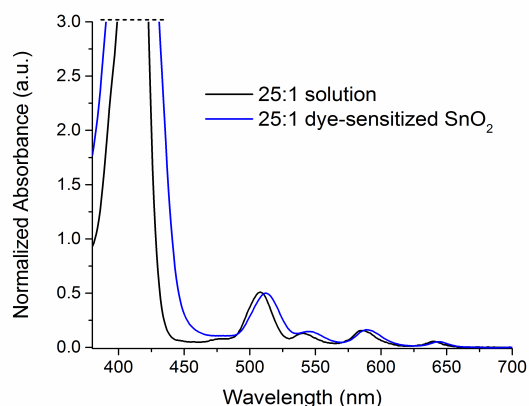


Figure S2. UV-visible spectra overlay of a 25:1 monomer-to-dyad ratio porphyrin solution in ethyl acetate (black) and the dry dye-sensitized SnO_2 film in air (blue).

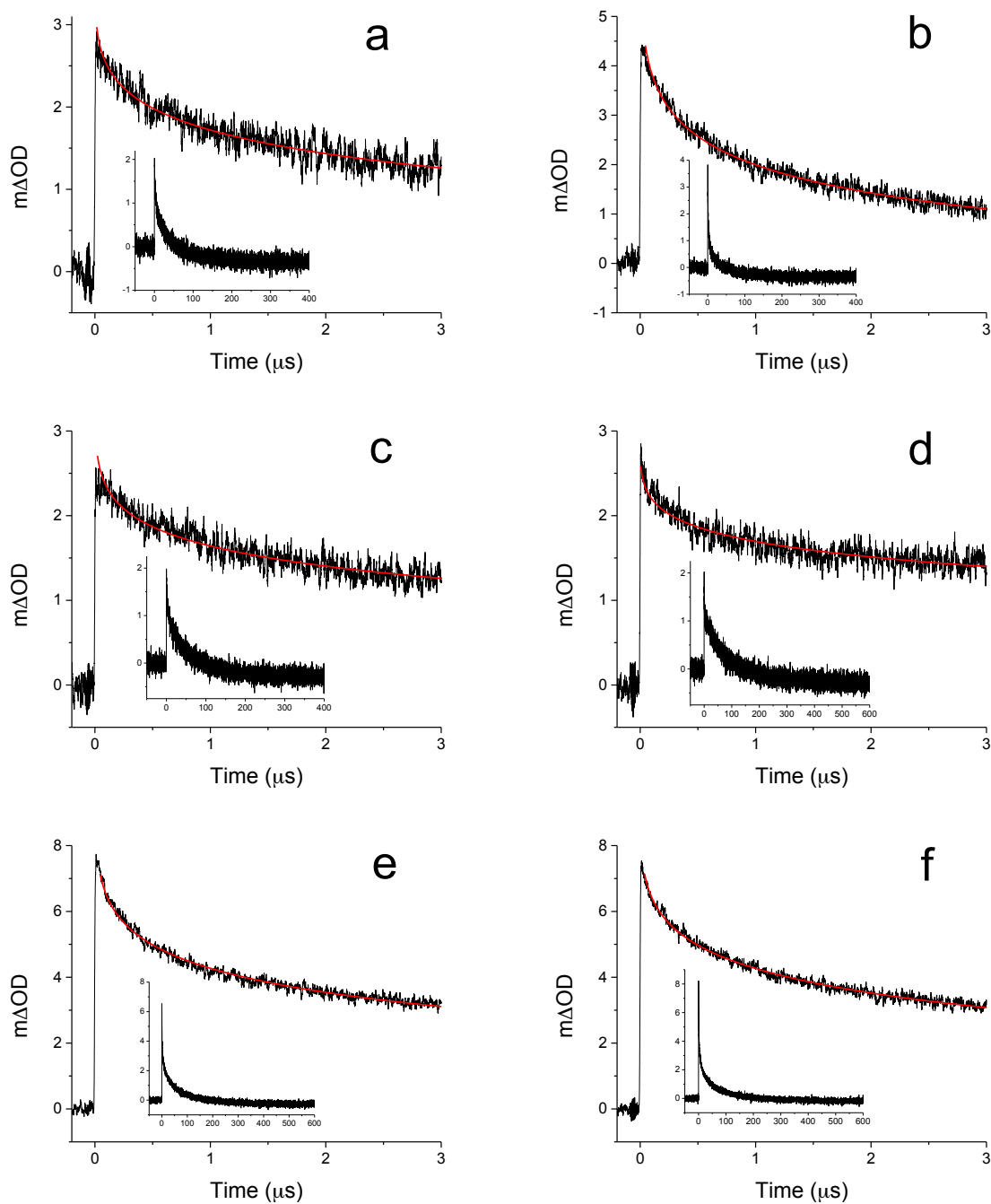


Figure S3. Transient absorption spectra for monolayers of pure monomer in: a) H_2O , b) 75% H_2O / 25% ACN, c) 50% H_2O / 50% ACN, d) 25% H_2O / 75% ACN, e) ACN, and f) PC. Solvents incorporated 100 mM LiClO_4 as electrolyte, with solvent mixtures as volume %. Stretched exponential decay fits are shown in red, and the decay parameters are found in Table 1 of the main text. Insets show longer timescales.

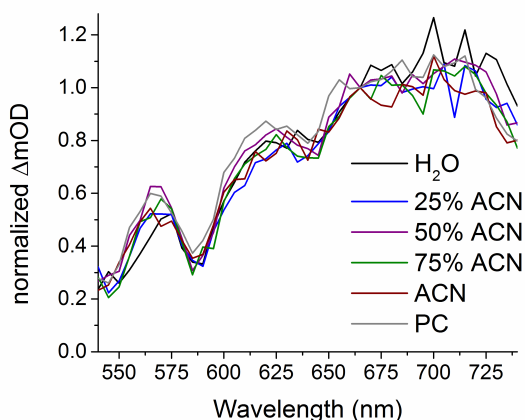


Figure S4. Transient absorption spectral map of monomer-sensitized SnO_2 electrodes in varying solvents containing 100 mM LiClO_4 . Data obtained at 2 μs after photoexcitation at 515 nm, and normalized at 665 nm.

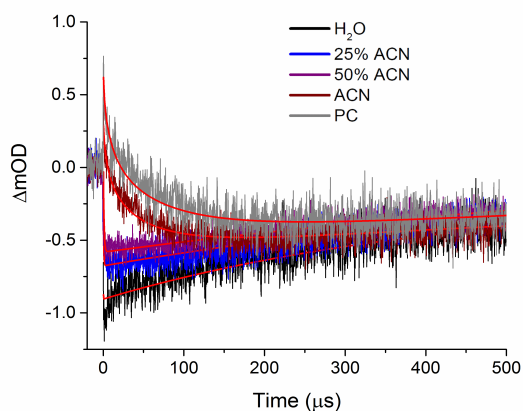


Figure S5. Transient absorption spectra of dye-sensitized SnO_2 electrodes with porphyrin monolayers containing a 25:1 monomer-to-dyad ratio in different solvents. Fits (red) were obtained using the model in the text and using kinetic parameters in Table 1 of the main text.

References

- (1) Brennan, B. J.; Durrell, A. C.; Koepf, M.; Crabtree, R. H.; Brudvig, G. W. Towards Multielectron Photocatalysis: A Porphyrin Array for Lateral Hole Transfer and Capture on a Metal Oxide Surface. *Phys. Chem. Chem. Phys.* **2015**, *17*, 12728-12734.
- (2) Antoniuk-Pablant, A.; Terazono, Y.; Brennan, B. J.; Sherman, B. D.; Megiatto, J. D.; Brudvig, G. W.; Moore, A. L.; Moore, T. A.; Gust, D. A New Method for the Synthesis of β -Cyano Substituted Porphyrins and Their Use as Sensitizers in Photoelectrochemical Devices. *J. Mater. Chem. A* **2016**, *4*, 2976-2985.